THE ASTROPHYSICAL JOURNAL, 462:L9–L12, 1996 May 1

STRONG REDSHIFT CLUSTERING OF DISTANT GALAXIES[1]

JUDITH G. COHEN,[2] DAVID W. HOGG,[3] MICHAEL A. PAHRE,[2] AND ROGER BLANDFORD[3]
Received 1994 January 16; accepted 1996 February 15

ABSTRACT

We present initial results from a redshift survey carried out with the Low Resolution Imaging Spectrograph on the 10 m W. M. Keck Telescope of a field 14.6 arcmin^2 in solid angle. In the redshift distribution of the 106 extragalactic objects in this sample we find five strong peaks, with velocity dispersions of $\sim$500 km s^{-1}. There is evidence for a nonuniform areal density of objects in at least two peaks. These peaks have characteristics (velocity dispersions, density enhancements, spacing, and spatial extent) similar to those of nearby galaxy structures (e.g., walls and clusters), and these are expected in a survey of this kind. We suggest that the prominence of these structures in our survey relative to that in other surveys can be attributed to our K selection and dense sampling.

Subject headings: cosmology: observations — galaxies: distances and redshifts — large-scale structure of universe

1. INTRODUCTION

This is the first in a series of papers describing the results of a deep survey of faint field galaxies in a single field centered at R. A. (J2000) $00^h53^m23^s.20$, decl. $+12°33'57''.5$. The field is from the *HST* Medium Deep Survey (Griffiths et al. 1994), randomly selected on the basis of high Galactic latitude ($b = -50°$) and low reddening ($A_V = 0.13$ mag; Burstein & Heiles 1982). Our redshifts were acquired with the Low Resolution Imaging Spectrograph (Oke et al. 1995) on the 10 m W. M. Keck Telescope over a rectangular strip 2×7.3 arcmin^2 extending north-south, centered on the *HST* field. Our primary sample comprises all 155 objects with $K < 20$ mag in the 2×7.3 arcmin^2 field. The photometry and the definition of the sample for spectroscopic work is described in Paper II of this series by Pahre et al. (1996). We reach higher galaxy surface densities than the *I*-selected Canada-France Redshift Survey (CFRS) survey (LeFèvre et al. 1995); our survey complements and extends to fainter objects the *K*-selected sample of the Hawaii group (Songaila et al. 1994).

Paper III in this series (Cohen et al. 1996) provides a detailed description of the redshift survey. Of the 155 objects in the sample, 90 have spectra typical of normal galaxies, three are quasars or broad-lined AGNs, and 19 are Galactic stars. Of the remaining objects, 35 were observed, but no redshift could be determined, and eight were not observed at all. The effects of incompleteness in the sample selection and redshift identification are discussed in Papers II and III; both are irrelevant for the present work. The median redshift z of the 93 extragalactic objects in the main sample is $z = 0.57$. An additional 13 galaxy redshifts were determined for objects in this field which were slightly fainter than the $K < 20$ mag limit or which lie slightly outside the spatial boundaries of the *K*-selected sample.

[1] Based in large part on observations obtained at the W. M. Keck Observatory, which is operated jointly by the California Institute of Technology and the University of California.

[2] Palomar Observatory, Mail Stop 105-24, California Institute of Technology.

[3] Theoretical Astrophysics, California Institute of Technology, Mail Stop 130-33, Pasadena, CA 91125.

2. REDSHIFT DISTRIBUTION

The redshift histogram is shown in Figure 1. Of the 106 objects, 40 are in the two strongest peaks, and 64 are in the 5 strongest, i.e., having $|z - z_p| < 0.020$ for $z_p = 0.392$, 0.429, 0.581, 0.675, and 0.766. In spite of the fact that there are no clusters apparent in the images of this field, the objects are highly clustered in redshift space. The overdensities in redshift space are at least a factor of 5, and more than 60% of the objects in the sample lie in these structures.

2.1. *Feature Significance*

We now consider the probability that these apparent features might arise by chance out of a smooth galaxy distribution. This significance calculation is performed not in redshift but in the quantity $V \equiv c \ln (1 + z)$. This coordinate is devoid of global meaning but, granted an overall Hubble expansion, corresponds incrementally to local velocity differences. The galaxies are contained in an interval $4 \times 10^4 < V < 2.4 \times 10^5$ km s^{-1}. As there is no adequate a priori understanding of the population from which these galaxies are drawn, the measured data set is used to derive smoothed velocity distributions by the addition of random velocity shifts drawn from a Gaussian distribution with width σ_V. This effectively erases the obvious structure without affecting the overall velocity distribution function. The data set is divided into N_b uniform velocity bins, and the number of galaxies n_{0i} is counted in the single bin centered on each of the candidate associations. This exercise is repeated using multiple realizations of the smoothed distribution; the mean $\bar{n}_i$ and standard deviation σ_{ni} are measured for each bin.

A measure of the significance of each feature is the statistic $X_i = |n_{0i} - \bar{n}_i|/\sigma_{ni}$. To test the null hypothesis that individual features arise by chance, we also measure the distribution of X_i in the smoothed redshift data. Finally, as the appearance of features like these is notoriously sensitive to the binning, we repeat this procedure with different values of N_b and, for each value of N_b, a range of shifts of bin "phase," comparing the maximum values of X_i measured with the maximal values produced from the smoothed distribution.

To carry this scheme out in practice, a conservatively small smoothing length $\sigma_V = 2 \times 10^3$ km s^{-1} was adopted, N_b ranged from 35 to 125 (in integer increments), and for each N_b, 10

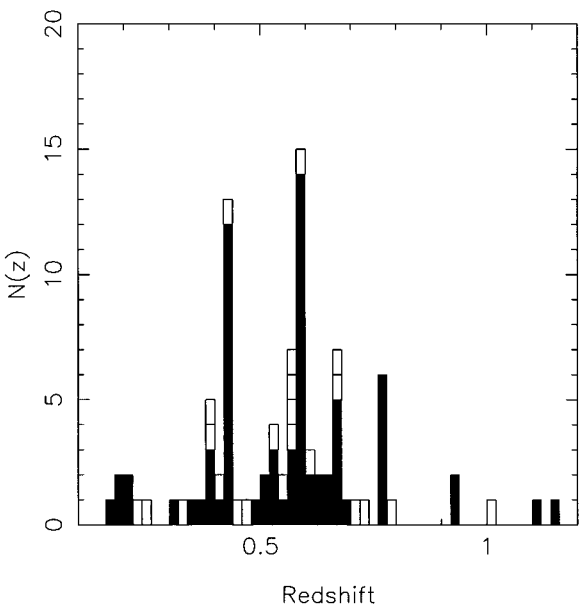

FIG. 1.—Redshift histogram for the galaxies in our survey. The filled columns denote galaxies whose redshifts are considered secure, while the open columns denote galaxies whose redshifts are of lower precision.

equally spaced values of bin phase shift from 0 to 1 bin width were allowed. For each value of these parameters, 1000 realizations of the Gaussian smoothed distribution were investigated. The results are given in Table 1, including the observed z_p, the number of galaxies within the bin coinciding with z_p (this number changes slightly depending on N_b; the value given is that corresponding to the N_b and phase at which X_i is the largest; it is not the same as the number assigned to each peak by the $|z - z_p| < 0.020$ rule), the largest value $X_{\max}$ of X_i for that feature inferred from the data seen over the full range in N_b and phase, and the likelihood of the feature arising by chance, computed as the fraction of realizations of the smoothed distribution in which such a large value of X_i was found in any bin. The latter quantity shows that the feature at $z = 0.392$ is not significant and the one at $z = 0.766$ is only marginally so. These results are robust to eliminating the few galaxies with redshifts of lower precision, or the 13 not in the K-selected sample. The estimated significances increase with increasing smoothing length σ_V.

2.2. *Velocity Dispersions*

The radial velocity precision of our redshifts is unusually high for a deep redshift survey. We estimate that the uncertainty in z for those objects with redshifts considered secure and accurate (comprising 80 of the 106 galaxies) is ≈300 km s^{-1}. The velocity dispersions for the five strongest peaks in the redshift histogram are given in Table 2. The velocity dispersions of the peaks are only slightly smaller when the objects with low-precision redshifts are excluded. Both because of the biasing effect of including outliers and the spreading of redshifts due to measurement uncertainties, these velocity dispersions should be treated as upper limits.

TABLE 1

STATISTICAL PARAMETERS FOR REDSHIFT PEAKS

z_p	Number of Galaxies at N_b (max)	$X_{\max}$	Likelihood
0.392.....	9	3.4	0.5
0.429.....	12	6.4	0.005
0.581.....	20	12.4	0
0.675.....	8	5.3	0.02
0.766.....	6	5.0	0.2

TABLE 2

VELOCITY DISPERSIONS IN REDSHIFT PEAKS

z_p	N[a]	$\sigma_v(N)$ (km s^{-1})	$\sigma_v(N-1)$[b] (km s^{-1})
0.392	9	585	465
0.429	17	685	615
0.581	23	610	410
0.675	8	440	405
0.766	7	975	670

[a] Number of galaxies with z within 0.02 of z_p.
[b] Omitting the most discrepant galaxy, velocity dispersion as derived from the remaining $N - 1$.

3. ANGULAR DISTRIBUTION

The angular distribution of the entire sample, as well as that of galaxies with $|z - z_p| < 0.020$ for each of the five peaks, is shown in Figure 2.

To provide a quantitative test of the uniformity of the areal distributions, two-dimensional Kolmogorov-Smirnov (K-S) tests (Fasano & Franceschini 1987) were applied to the sample. When the areal distribution of the entire sample is compared with a uniform distribution, no evidence for nonuniform distribution is found. For each feature, the areal distribution of objects in the feature (membership defined by maximizing X_i as described in the previous section) is compared with that of all the objects not in the feature. The two-dimensional K-S test D-values for the individual peaks are given in Table 3. Two, at $z = 0.392$ and $z = 0.581$, are significantly nonuniform in areal distribution. These results are not significantly altered if one uses only the 93 objects in the $K < 20$ mag sample. They are also robust to replacing the distribution of feature nonmembers with a uniform distribution.

Interestingly, the one feature, at $z = 0.392$, judged insignificant in redshift clustering shows significant angular clustering, and the feature, at $z = 0.766$, judged marginally significant in redshift clustering, is also marginally significant in angular clustering. For this reason we judge both these features at least marginally significant.

4. DISCUSSION

4.1. *Effects of Sample Definition Decisions*

Although there are many other faint object redshift surveys, none have found as much strong redshift clustering as is presented here. We believe that this can be attributed to differences in sample definition. This survey of objects goes to high galaxy number density, 4×10^4 deg^2 at $K = 20$, comparable to the Hawaii survey (Songaila et al. 1994) but with greater completeness at the faint end, and deeper than the CFRS (LeFèvre et al. 1995) or the B-selected LDSS-2 survey (Glazebrook et al. 1995). Infrared selection is not subject to the same biases toward late-type spirals and irregulars as is found in B-selected samples. Our redshifts are measured with good precision, allowing good resolution of the peaks and their velocity dispersions.

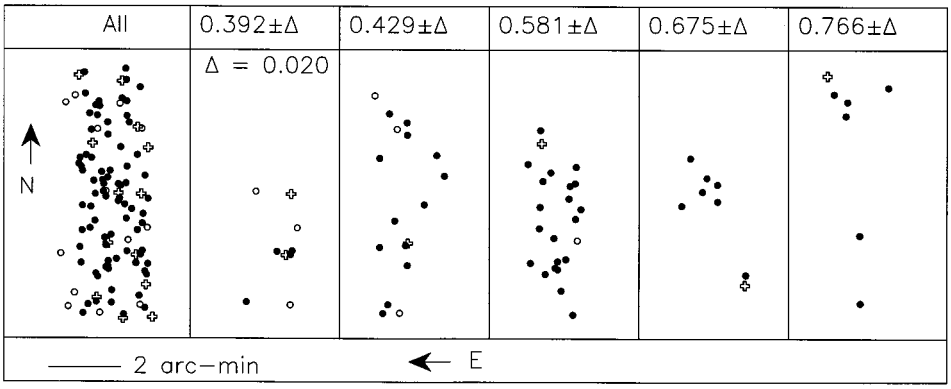

FIG. 2.—Distribution of our sample of galaxies projected onto the sky is shown. The first panel shows the entire sample. This is followed by the spatial distribution of the galaxies in each of the five strongest peaks in the redshift histogram. Galaxies not included in the $K < 20$ mag sample are shown as open circles, while those with uncertain z are shown as open crosses.

Finally and most importantly, this sample is not sparsely sampled, i.e. (almost), every object with $K < 20$ mag in the field is observed, so we do not miss structures of limited angular extent. For very sparsely sampled data, one obtains no statistically valid peaks at all in the redshift distribution; cf. the CFRS (Lilly et al. 1995). As one samples less sparsely, "walls" with substantial velocity dispersions, as in the ESO survey (Bellanger & de Lapparent 1995), appear. Suggestions similar to these regarding the effect of different sampling schemes have been offered by de Lapparent, Geller, & Huchra (1991) and by Ramella, Geller, & Huchra (1992) to explain why some redshift surveys did not see structures such as the Great Wall, while others, e.g., the CfA survey (de Lapparent, Geller, & Huchra 1986), did.

4.2. *Structure Morphology*

In general, imaging surveys for galaxy structures find clusters and filaments because these appear as angular patches of higher projected number density, but do not find walls because the projected number density is relatively invariant to collapse from three-dimensional volumes into two-dimensional walls. On the other hand, redshift surveys like this one, in small angular areas, are unlikely to hit compact clusters and filaments but should pierce any walls. Because the structures in the present sample are seen in the redshift distribution but not in the imaging, there is some evidence that they are wall-like.

The derived velocity dispersions σ_v are small and reminiscent of those of sparse clusters of galaxies. Zabludoff, Huchra, & Geller (1990) found a median $\sigma_v = 740$ km s^{-1} for 69 nearby moderately rich Abell clusters. Our observed values of σ_v are much smaller than that found for superclusters; for example, Postman, Geller, & Huchra (1988) found $\sigma_v = 1300$ km s^{-1} for primary members of the seven Abell clusters in the Corona Borealis supercluster, while Small (1996) found 1800 km s^{-1} for the entire supercluster. If the cluster Cor Bor itself is excluded, then the value drops to less than 1000 km s^{-1} (Postman, Huchra, & Geller 1992; Zucca et al. 1993). Small (1996) also observed many individual lines of sight through the supercluster and found 400 km s^{-1} $< \sigma_v <$ 1200 km s^{-1}; these lines of sight are comparable in extent to our field, while our derived σ_v are among the lowest values measured along individual Cor Bor lines of sight. The velocity dispersion for the Great Wall, however, is 230 km s^{-1} measured over 3° cells (Ramella et al. 1992), while that for groups in the SSRS2 (Da Costa et al. 1994) is ~200 km s^{-1}. Our σ_v are thus comparable to Great Wall–size structures, poor clusters of galaxies, or lines of sight through superclusters. The separations between structures are also comparable: the comoving distances of the five strongest redshift peaks are 915, 981, 1228, 1364, and 1485 h^{-1} Mpc, while the distance between the Cor Bor supercluster and the one immediately behind it at $z \approx 0.12$ (Gioia et al. 1982; Sarazin, Rood, & Struble 1982; Small 1996) is 130 h^{-1} Mpc. In this regard our redshift distribution is also reminiscent of that found by Broadhurst et al. (1990), although the features in ours are not "periodic."

At $z = 0.6$, our field has a size of 1.7×0.5 h^{-2} Mpc^2. We take the number density of clusters in the universe to be of the order of a few times 10^{-5} h^{-3} Mpc^{-3}, as reported for Shectman (1985) clusters (Bahcall 1988) and $R \geq 1$ Abell galaxy clusters (Postman et al. 1996). The fact that we observe five clusters along a randomly selected line of sight implies a typical cluster radius of between 2–5 h^{-1} Mpc, depending on the exact number density and the world model. These lengths are on the order of, if a bit higher than, locally measured cluster radii, and are consistent with the marginally nonuniform angular distributions we find above. That these structures might be sparse clusters is also consistent with their small measured velocity dispersions.

If we "run the clock backward" on structure formation, it seems unlikely that the huge walls and rich clusters seen locally would completely disperse into a uniform galaxy distribution by redshift of 1. It would be surprising if the high-redshift counterparts of local walls were *not* found in deep redshift surveys. (Rich clusters, on the other hand, only contain a small fraction of all galaxies and are much less likely to be encountered.) Many groups have found similar or related structures.

TABLE 3

RESULTS OF TWO-DIMENSIONAL K-S TESTS FOR UNIFORM SPATIAL DISTRIBUTION

z_p	Number of Galaxies at N_b (max)	Two-dimensional K-S Statistic D
0.392	9	0.01
0.429	12	0.2
0.581	20	0.01
0.675	8	0.4
0.766	6	0.1

Bellanger & de Lapparent (1995), presenting the first results of the ESO Sculptor Faint Galaxy Redshift Survey for galaxies with $R < 20.5$ mag 0.28 deg^{-2}, have found what they call "walls" analogous to the Great Wall seen in the local universe. The galaxy distribution they see is strongly clustered in the line of sight, consisting of walls and voids, although their redshift histogram does not show structures as strongly peaked in redshift space as those presented here (for the reasons given above). A structure interpreted as a normal dense galaxy cluster at high redshift was found by LeFèvre et al. (1994), consisting of a group of 12 galaxies around a quasar at $z = 0.98$, with velocity dispersion $\sigma_v = 955$ km s^{-1} and transverse structure on a characteristic scale $2\,h^{-1}$ Mpc. Of course an observation of transverse structure is not an argument against wall morphology because, if a sheet becomes self-gravitating, it must break up into structures that are as wide as the wall is thick (Ostriker & Cowie 1981). Hutchings, Crampton, & Johnson (1995) have detected compact groups of galaxies with a radius of $\sim 1'$ ($0.25\,h^{-1}$ Mpc) around 14 QSOs with $z \sim 1.1$. Ellingson, Green, & Yee (1991, see also Ellingson & Yee 1994) find galaxy clusters around QSOs with $\sigma_v \sim 400$–500 km s^{-1}. Studies of quasar absorption lines in QSO pairs and in individual objects also suggest the existence of superclusters at $z \approx 2.5$ (Dinshaw & Impey 1996).

4.3. *Critical Future Observations*

Given these observations and our interpretation, it is possible to predict the outcome of future observations which are crucial in determining the statistical, morphological, and physical properties of these structures. If they are wall-like, then we expect to see coherence as we extend the survey to adjacent fields. Even if the clumps are sparse clusters, local observations of Cor Bor and the Great Wall suggest that the clumps will group into large two-dimensional sheets. Redshift surveys in adjacent fields are essential to answering these questions of morphology.

There are many redshift surveys undertaken by different groups, and it is important to demonstrate that the differences among these surveys in prominence of structures in the z distribution are indeed attributable to differences in sample definition. It is imperative that the objects in this survey (and adjacent fields) be reselected with photometric and sparse-sampling criteria matched to other surveys; comparison could then be used to confirm that the structures are common and this field is not "special." Also, the morphology-density relation (Dressler 1980) suggests that changing to bluer selection bands should reduce the percentage of galaxies lying inside the structures.

Finally, similar samples in widely separated fields will provide us with statistics for these structures, such as typical separations, velocity dispersions, filling factor, etc. It is possible that some of the much discussed field-to-field variations found in galaxy counts, angular correlation functions, and redshift distributions (e.g., Koo & Kron 1992) can be attributed to the field-to-field variations in the walls along the line of sight.

If, as we strongly suspect they will, further observations do substantiate the view that roughly half the old galaxies are localized in walls, then a major challenge will be to determine whether the galaxies in these walls have virialized. At present there appear to be no good observational arguments against this view.

We are grateful to George Djorgovski, Keith Matthews, Gerry Neugebauer, Tom Soifer, and Jim Westphal for helpful conversations and to Todd Small and Wal Sargent for permission to use their data on Cor Bor prior to publication. The entire Keck user community owes a huge debt to Bev Oke, Jerry Nelson, Gerry Smith, and many other people who have worked to make the Keck Telescope a reality. We are grateful to the W. M. Keck Foundation, and particularly its president, Howard Keck, for the vision to fund the construction of the W. M. Keck Observatory.

REFERENCES

Bahcall, N. A. 1988, ARA&A, 26, 631
Bellanger, C., & de Lapparent, V. 1995, ApJ, 455, L103
Broadhurst, T., Ellis, R., Koo, D., & Szalay, A. 1990, Nature, 343, 726
Burstein, D., & Heiles, C. 1982, AJ, 87, 1165
Cohen, J. G., et al. 1996, in preparation (Paper III)
Da Costa, N., et al. 1994, ApJ, 424, L1
de Lapparent, V., Geller, M., & Huchra, J. P. 1986, ApJ, 302, L1
———. 1991, ApJ, 369, 273
Dinshaw, N., & Impey, C. D. 1996, ApJ, 458, 73
Dressler, A. 1980, ApJ, 236, 351
Ellingson, E., Green, R. F., & Yee, H. K. C. 1991, ApJ, 378, 476
Ellingson, E., & Yee, H. K. C. 1994, ApJS, 92, 33
Fasano, G., & Franceschini, A. 1987, MNRAS, 225, 155
Glazebrook, K., Ellis, R., Colless, M., Broadhurst, T., Allington-Smith, J., & Tanvir, N. 1995, MNRAS, 273, 157
Gioia, I. M., Geller, M. J., Huchra, J. P., Maccarao, T., Steiner, J. E., & Stocke, J. 1982, ApJ, 255, L17
Griffiths, R. E., et al. 1994, ApJ, 437, 67
Hutchings, J. B., Crampton, D., & Johnson, A. 1995, AJ, 109, 73
Koo, D. C., & Kron, R. G. 1992, ARA&A, 30, 613
LeFèvre, O., Crampton, D., Lilly, S. J., Hammer, F., & Tresse, L. 1994, ApJ, 423, L89
———. 1995, ApJ, 455, 60
Lilly, S. J., LeFèvre, O., Crampton, D., Hammer, F., & Tresse, L. 1995, ApJ, 455, 50
Oke, J. B., et al. 1995, PASP, 107, 3750
Ostriker, J., & Cowie, L. L. 1981, ApJ, 243, L127
Pahre, M. A., et al. 1996, in preparation (Paper II)
Postman, M., Geller, M., & Huchra, J. P. 1988, AJ, 95, 267
Postman, M., Huchra, J. P., & Geller, M. J. 1992, ApJ, 384, 404
Postman, M. A., Lubin, L. M., Gunn, J. E., Oke, J. B., Hoessel, J. G., Schneider, D. P., & Christensen J. A. 1996, ApJ, 111, 615
Ramella, M., Geller, M. J., & Huchra, J. P. 1992, ApJ, 384, 396
Sarazin, C., Rood, H., & Struble, M. 1982, A&A, 108, L7
Shectman, S. 1985, ApJS, 57, 77
Small, T. A. 1996, Ph.D. thesis, Caltech
Songaila, A., Cowie, L. L., Hu, E. M., & Gardner, J. P. 1994, ApJS, 94, 461
Zabludoff, A. I., Huchra, J. P., & Geller, M. J. 1990, ApJS, 74, 1
Zucca, E., Zamorani, G., Scaramella, R., & Vettolani, G. 1993, ApJ, 407, 470